



Effect of testing conditions and filtration mechanisms on SDI

A. Alhadidi^a, B. Blankert^b, A.J.B. Kemperman^{a,*}, J.C. Schippers^c, M. Wessling^a, W.G.J. van der Meer^a

^a Membrane Technology Group, Faculty of Science and Technology, University of Twente, P.O. Box 217, 7500 AE Enschede, The Netherlands

^b Norit X-Flow, P.O. Box 741, 7500 AS, Enschede, The Netherlands

^c UNESCO-IHE Delft, Westvest7, P.O. Box 3015, 2601 DA Delft, The Netherlands

ARTICLE INFO

Article history:

Received 24 December 2010

Received in revised form 10 June 2011

Accepted 14 July 2011

Available online 22 July 2011

Keywords:

Silt Density Index

Fouling mechanisms

Testing conditions

Mathematical models

ABSTRACT

The Silt Density Index is applied world-wide for many decades to determine the fouling potential of feed water of reverse osmosis systems and more recently to judge the performance of micro- and ultrafiltration systems. However there are growing doubts about the reproducibility and accuracy of this test.

Currently, the Silt Density Index (SDI) is applied without any correction for temperature, applied pressure and membrane resistance. Besides that, the SDI is not based on any fouling mechanism which affects its reproducibility and accuracy.

To identify opportunities for improvements, existing mathematical fouling models were further extended to study the effect of temperature, applied pressure and membrane resistance on the SDI value under four different fouling mechanisms. Significant variations in SDI values are observed mathematically as a result of differences in temperature and membrane resistance for the same water quality. The fouling mechanisms are described by the relationship between the filtrated volume w and the total resistance R . The sensitivity of the SDI for variations in the testing parameters theoretically increases when the relation between w and R is stronger.

The SDI increases with an increase in feed temperature and applied pressure. Temperature has a substantial effect on SDI. As a consequence it is not recommended to compare SDI values measured at different temperatures. The SDI value decreases when membranes with a high resistance are used. To achieve a more reliable SDI, the use of a standardized membrane with constant properties, in particular having a narrow resistance range, is recommended.

© 2011 Elsevier B.V. All rights reserved.

1. Introduction

Reverse osmosis RO membrane systems are widely used in the desalination of water. However, fouling phenomena in these systems remains a challenge. Four main different fouling types are identified [1–7]: (1) particulate fouling due to suspended and colloidal matter, (2) biofouling due to adhesion and subsequent growth of bacteria, (3) organic fouling due to organic compounds and (4) scaling due to precipitation of sparingly soluble compounds.

Membrane fouling may manifest in deposition/growth on membrane surface and/or spacers in spiral wound membrane elements. Fouling of membrane surfaces, results in increasing hydraulic resistances and reduced rejection, due to concentration polarization in the foul layer. Deposition and/or bacterial growth on membrane spacers result in increasing pressure drop and eventually in membrane damage. Remedial actions are commonly taken e.g. regular chemical cleaning of the membrane elements. However frequent cleaning will shorten the life time of the membranes.

This article focuses particulate fouling; in particular on the measurement of the fouling potential of reverse osmosis feed water, due to colloidal and suspended matter.

In practice, the SDI is used most often and has been applied worldwide for many decades [8]. The main advantage of the SDI test is that the test is simple to execute even by non-professionals.

It has been developed to determine the fouling potential of the hollow fine fiber Permasep Permeators of Dupont. Later on this test has been adopted by manufacturers of spiral wound elements as well.

During the SDI test the time required to filter a fixed volume of water through a standard microfiltration membrane at a constant given pressure is measured. The difference between the initial time and the time of a second measurement after 15 min (after silt built-up) results in the SDI value [9]. The ASTM describes this test as a standard test for RO fouling potential due to particles. According to the standard, the applied pressure is 207 ± 7 kPa (30 ± 1 psi). The water temperature must remain constant (± 1 °C) throughout the test.

This test is commonly used to judge the performance of pre-treatment systems – including micro- and ultrafiltration – as well. It has the status of ultimate tool in predicting membrane fouling.

* Corresponding author. Tel.: +31 53 4892956; fax: +31 53 4894611.

E-mail address: a.j.b.kemperman@utwente.nl (A.J.B. Kemperman).

However doubts are growing about the real predictive value of this test, because poor reproducibility is frequently reported from practice. This poor reproducibility might be related to the facts that it [10,11]:

- has no linear relation with the concentration of colloidal/suspended matter;
- an empirical test, which is not based on any filtration mechanism;
- is not corrected for temperature, pressure and membrane properties e.g. permeability.

In addition artifacts might play a role as well e.g. such as air bubbles in the equipment and operator inaccuracies.

Besides the reported poor reproducibility, doubts are growing about the predictive value of the SDI as well. These doubts are based on the inability to capture small particles, which might foul RO membranes, having much smaller pores than 0.45 μm . For this purpose the MFI (0.05) and MFI-UF has been developed [7,10–14]. The applicability of these tests in predicting fouling of RO membranes will not be discussed.

To overcome the main deficiencies of this test the Modified Fouling Index (MFI0.45) has been developed [10]. This index is based on cake filtration; it is corrected for temperature and pressure and shows a linear relation with the concentration of colloidal/suspended matter. Unfortunately measuring MFI is much more complicated than SDI. Consequently it is not suitable for operators, which is a serious disadvantage. So it is useful to identify opportunities to improving the SDI test with respect to reproducibility and accuracy.

The objective of this study is to investigate the influence of temperature, pressure and membrane resistance on SDI, assuming four different fouling mechanisms namely:

- cake filtration;
- intermediate blocking;
- standard blocking;
- complete blocking;

For this purpose theoretical models are developed and applied to simulate different test conditions. The results of these simulations are compared with experimental tests, making use of aluminum oxide particles (0.6 μm) as model colloid.

2. Theory and background

2.1. SDI definition

To determine the SDI, the rate of plugging of a membrane filter with pores of 0.45 μm at 207 kPa is measured. The measurement is done as follows;

- (a) The time t_1 is determined which is required to filter the first 500 mL.
- (b) 15 min (t_f) after the start of this measurement time t_2 is measured which is required to filter 500 mL.
- (c) The index is calculated with the following formula.

$$\text{SDI} = \frac{100\%}{t_f} \left(1 - \frac{t_1}{t_2} \right) = \frac{\%P}{t_f} \quad (1)$$

where SDI is the Silt Density Index (%/min), t_1 is the time required to collect the first volume (e.g. 500 mL), t_2 is the time required to collect the second volume (500 mL) and t_f is the time of the second measurement (15 min). If plugging ratio (%P) is exceeding 75% a shorter period t_f has to be taken, e.g. 10, 5 or 2 min.

2.2. Fouling model

The influence of performing an SDI test under different fouling mechanisms such as cake filtration or pore blocking will be studied. Hermia [15] described four empirical models that corresponded to four basic types of fouling: complete blocking, intermediate blocking, standard blocking and cake layer formation. The parameters considered by these models have a physical meaning and contribute to the comprehension of the mechanisms of membrane fouling. These models were developed for dead-end filtration and are based on constant pressure filtration laws. The four fouling models are summarized in Table 1, where: [16]

w_R : represents the specific cake resistance and is defined as the volume of feed water per unit area for which the cake resistance is equal to the membrane resistance.

w_A : represents the pore blocking potential and is defined as the volume of feed water per unit area that contains enough particles to block the pores completely.

w_V : represents the pore filling potential and is defined as the amount of feed water per unit area that contains enough particles to fill the pores completely.

Based on the definitions given above, the fouling parameters $w_{(R,A,V)}$ are inversely proportional to the particle concentration. For example, one will need half amount of feed water if the amount of particles in the feed water is doubled to block all the pores or to build up a cake layer.

The membrane resistance R_M cannot change without changing: pore size distribution, number of pores, pore length, tortuosity and hydrophilicity. Fouling is a result of interaction between the membrane and feed water. Thus, membrane resistance is in practice hard to vary independently.

If it is assumed that the retention does not change, the specific cake resistance is not affected by the membrane properties. One should be careful however, since w_R is defined relative to the membrane:

$$w_R = \frac{R_M}{R_C} \quad (2)$$

where R_M is the membrane resistance and R_C is the cake resistance.

The pore blocking mechanisms (complete, intermediate, standard) are directly related to the pore volume and area. If it is assumed that the membrane resistance can be varied without changing the volume and area of the pores, it follows that $w_{A,V}$ are independent parameters.

Assuming constant retention, for dead-end filtration and an initially clean membrane, the fouling state is defined by:

$$\frac{dw}{dt} = J \quad (3)$$

in which J is the filtration flux and w is the filtration state (filtrated volume per unit area).

Blankert et al. [16] generalized the relations between the total resistance and the filtrated volume for each of the four fouling mechanisms, by writing the equations in a common form:




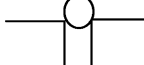
$$\frac{dR}{dw} = C \cdot R^m \quad (4)$$

R is the total resistance, and C and m are constants depending on the filtration mechanisms. Table 1 shows the resulting resistance R as a function of the filtration state w , the membrane resistance R_M and the fouling potential of the feed.

The resistance R is calculated using Darcy's law [17]:

$$R = \frac{\Delta P}{\mu \times J} \quad (5)$$

Table 1
Definition of the four fouling mechanisms. The parameters C and m related to the fouling mechanisms and particle concentration. Total resistance R as function of filtration state w [16].

Mechanism	Definitions	m	C	Resistance equation $R(w)$
Cake filtration		0	$\frac{R_M}{w_R}$	$R_M \left(1 + \frac{w}{w_R}\right)$
Intermediate blocking		1	$\frac{1}{w_A}$	$R_M \cdot e^{w/w_A}$
Standard blocking		1.5	$\frac{2}{w_V R_M^{0.5}}$	$R_M \left(1 - \frac{w}{w_V}\right)^{-2}$
Complete blocking		2	$\frac{1}{w_A R_M}$	$R_M \left(1 - \frac{w}{w_A}\right)^{-1}$

The relative difficulty of operation (γ) due to membrane fouling was introduced by Blankert et al. [16]. Conceptually, the difficulty of operation is the ratio between the total resistance and the membrane resistance:

$$\gamma = \frac{R}{R_M} \quad (6)$$

where R is the total resistance and R_M is the membrane resistance.

The trajectory of this variable can be calculated from the fouling model parameters (C and m) and the operating strategy parameters. The values for s equal to 0, 1 and 0.5 define constant flux, constant pressure and constant power filtration, respectively. The relative difficulty of operation in time is given by [16]:

$$\gamma(t) = \begin{cases} (1 + (s - m + 1)K_0 \cdot t)^{1/(s-m+1)} & s - m + 1 \neq 0 \\ e^{K_0 \cdot t} & s - m + 1 = 0 \end{cases} \quad (7)$$

where the parameter K_0 is defined as:

$$K_0 = C \cdot J_0 \cdot R_M^{m-1} = \frac{C \cdot \Delta P \cdot R_M^{m-2}}{\mu} \quad (8)$$

with J_0 as the initial flux and μ as the water viscosity.

The state trajectory may be given by:

$$w(t) = \begin{cases} \frac{1}{C} \frac{R_M^{1-m}}{1-m} (\gamma^{1-m} - 1) & 1 - m \neq 0 \\ \frac{1}{C} \ln(\gamma) & 1 - m = 0 \end{cases} \quad (9)$$

2.3. ASTM standard

In the most recent ASTM International 'Standard Test Method for Silt Density Index (SDI) of Water' [9] the following membrane properties are recommended to be used in the test:

Membrane white hydrophilic, mixed cellulose nitrate (50–75%) and cellulose acetate (MCE); mean pore size 0.45 μm . Diameter 47 mm nominal, plain; size 25 mm or 90 mm diameter also can be used. Thickness is between 115 and 180 μm . Pure water flow time 25–50 s for 500 mL under applied pressure difference 91.4–94.7 kPa. Bubble point 179–248 kPa; use only filters that are packaged in the same orientation.

If the plugging ratio % P is exceeding 75% a shorter period t_f has to be taken e.g. 10, 5 or 2 min.

3. Material and methods

The procedure for measuring the SDI will be described using our lab scale SDI setup. The MF membrane and model feed water will be listed, as well as the reference testing condition parameters will be defined. Besides that, the particle size distribution measurements protocol will be described.

3.1. SDI setup

The procedure for measuring the SDI has been standardized by ASTM [9]. Equipment and procedures used are as follows:

The apparatus was assembled as shown in Fig. 1. The feed pump was automatically controlled to provide a constant feed pressure of 207 ± 7 kPa (30 ± 1 psi). Before installing the membrane filter, the water to be tested was flushed through the apparatus in order to remove entrained contaminants. The water temperature was measured and kept constant throughout the test. An MF 0.45 μm membrane filter (25 mm in diameter) was placed on the support plate of the holder. The membrane filter was touched only with tweezers to avoid puncturing or contamination. It was checked whether the O-ring was in a good condition and properly placed. The trapped air was bled out through a relief air valve in the filter holder. The flow rate was measured using the flow meter (connected to a PC). The time to collect the first sample t_1 and the second sample t_2 were determined experimentally using the collected filtration data (time vs. volume). The SDI was calculated using Eq. (1).

From the raw filtration data obtained from the SDI setup, the resistance and filtered volume were calculated. Subsequently C , m and R_M are model parameters were determined by least-squares curve fitting [18], minimizing the following error criterion:

$$\min \sum_{i=0}^n (R(w_i, R_M, C, m) - R_i)^2 \quad (10)$$

where R total resistance, n is the number of data points, w_i is the accumulated filtrated volume per unit area and R_i is the total resistance at data point i .

3.2. Membrane

In accordance with the ASTM standard MF membrane material for SDI, commercial 0.45 μm cellulose acetate membranes (coded M7) were used (SterliTech CA045). The pore size

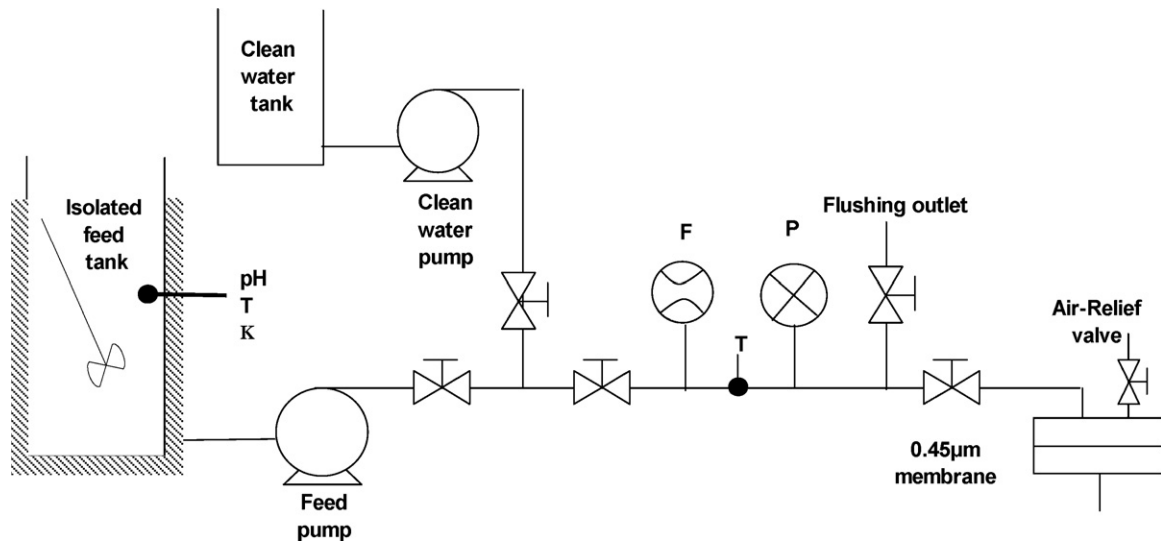


Fig. 1. Flowsheet of the SDI setup. Feed tank is shown. pH, Temperature (T) and conductivity (κ) are measured in the feed tank. Pressure (P), flow rate (F) and temperature (T) are measured in the feed line.

distribution of membrane M7 was measured using a Coulter Porometer II (VD3) with pore wetting liquid Profil3 using standard procedures described by the manufacturer. The capillary constant was set to the European System ($\tau = 1$).

3.3. Colloidal suspension as model water

To prepare the model feed water, hydrophilic α -Alumina particles (AKP-15, Sumitomo Chemical, Tokyo, Japan) with a core particle size of $0.6 \mu\text{m}$ and an isoelectric point (IEP) at pH 9 [19] were used. The AKP-15 particle has a narrow size distribution curve. The feed solution was prepared by adding 4 mg/L AKP-15 to demineralized water, purified by an Ultra-Pure system from Millipore (Synergy SYNS). The solution was well mixed using a mechanical mixer in the feed tank.

Malvern Instruments' Zetasizer range with Dynamic Light Scattering (DLS) was used to measure the α -alumina particle size distribution. To avoid the agglomeration of the particles, the pH was adjusted to 4.1 by adding HNO_3 .

3.4. Defined reference testing parameters

Membrane resistance, feed temperature, applied pressure and membrane area are the main testing parameters in this study. In order to study the effect of each parameter independently, the reference testing parameters were defined as:

- The membrane resistance R_M : in the updated version of the ASTM standard 2007, the membrane filter was more specified. The pure water flow time should be 25–50 s/500 mL under applied pressure 91.4–94.7 kPa. The calculated membrane resistance R_M can be obtained 0.86×10^{10} to $1.72 \times 10^{10} \text{ m}^{-1}$. The average value $R_M = 1.29 \times 10^{10} \text{ m}^{-1}$ will be defined as a reference membrane resistance.
- Feed temperature T : the lab temperature was taken as a reference feed temperature $T_o = 20^\circ\text{C}$.
- Applied pressure ΔP : the standard applied pressure $\Delta P_o = 207 \text{ kPa}$ was defined in this study as a reference pressure.
- Membrane area A_M : the diameter 47 mm was considered as standard membrane size and the membrane area $A_{M0} = 13.4 \times 10^{-4} \text{ m}^2$.

- SDI_o: the SDI limitation for the RO feed water SDI = 3 was defined as a target value.

4. Results and discussion

The SDI sensitivity for the variation in the particle concentration and the testing parameters will be described in this section. The theoretical results will be confirmed experimentally using a AKP-15 model feed water.

4.1. Mathematical model

Based on Eq. (9), the accumulated volume can be defined as $V(t) = w(t) \times A_M$. The SDI is determined under constant pressure, and therefore s is equal to 1. The filtrated volume V can be calculated by substituting Eq. (8) and Eq. (7) into Eq. (9) and results in Eq. (11):

$$V(t) = \begin{cases} \frac{A_M \cdot R_M^{1-m}}{C \cdot (1-m)} \left(\left(1 + \frac{(2-m) \cdot C \cdot \Delta P \cdot R_M^{m-2} t}{\mu} \right)^{(1-m)/(2-m)} - 1 \right) & m \neq 1, 2 \\ A_M \cdot w_A \ln \left(1 + \frac{\Delta P \cdot t}{w_A \cdot \mu \cdot R_M} \right) & m = 1 \\ A_M w_A (1 - e^{-\Delta P \cdot t / (w_A \cdot \mu \cdot R_M)}) & m = 2 \end{cases} \quad (11)$$

The time t to collect filtration volume V can be calculated by inverting Eq. (11):

$$t(V) = \begin{cases} \frac{\mu}{(2-m) \cdot C \cdot \Delta P \cdot R_M^{m-2}} \left(\left(\frac{V \cdot C \cdot (1-m)}{R_M^{1-m} \cdot A_M} + 1 \right)^{(2-m)/(1-m)} - 1 \right) & m \neq 1, 2 \\ (e^{V/w_A A_M} - 1) \cdot \frac{R_M \cdot w_R \cdot \mu}{\Delta P} & m = 1 \\ \ln \left(\frac{A_M \cdot w_A}{A_M \cdot w_A - V} \right) \cdot \frac{R_M \cdot w_A \cdot \mu}{\Delta P} & m = 2 \end{cases} \quad (12)$$

4.2. Calculating SDI

Eqs. (11) and (12) can be combined to give the analytical expression for the SDI, which is given in Annex 1.

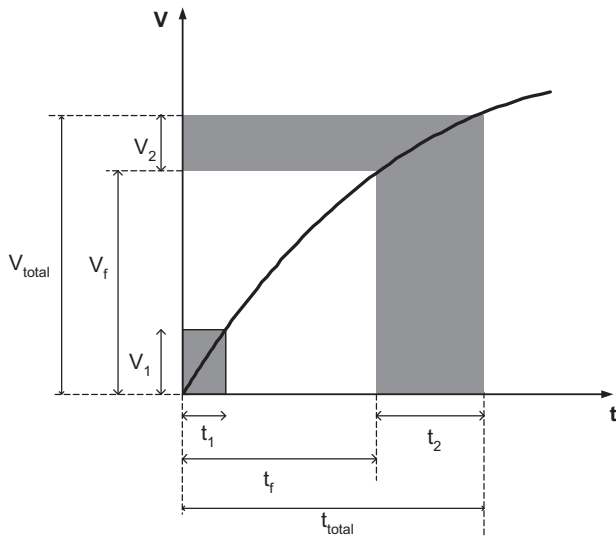


Fig. 2. Theoretical diagram showing the filtrated volume as function of time and the variables used to determine SDI.

With the functions $t(V)$ and $V(t)$, t_1 and t_2 can be determined which are needed to calculate the SDI (Eq. (1)):

$$\begin{aligned} t_1 &= t(V_1) \\ V_{15} &= V(t_{15}) \\ t_{\text{total}} &= t(V_{15} + V_2) \\ t_2 &= t(V_{15} + V_2) - t(V_{15}) \end{aligned} \quad (13)$$

These parameters are derived from Eqs. (11) and (12) using the following steps;

1. t_1 follows from Eq. (12)
2. t_2 cannot be determined directly and as a consequence a couple of steps are needed.
3. $V_{\text{total}} = V_f + V_2$ (V_{total} , V_f and V_2 are the volumes filtered in respectively t_{total} , t_f and t_2)
4. Substitution of t_f for t in Eq. (11) obtains V_f
5. Substitution of V_f in Eq. (12) gives t_f
6. t_2 follows from $t_2 = t_{\text{total}} - t_f$
7. The SDI is calculated by substitution of t_1 and t_2 in Eq. (1).

The filtrated volume as function of time (V vs. t) can plotted in a typical fouling curve as schematically presented in Fig. 2. Additionally, Fig. 2 illustrates schematically the determination steps for SDI from a time-volume curve.

4.3. Theoretical SDI sensitivity

An ideal fouling index should have a linear relationship with the relevant particle concentration in the feed water and should not be sensitive for the testing condition parameters nor the membrane resistance. It should have a linear relationship with the fouling potential. The sensitivity of the SDI results for particle concentration and testing parameters such as feed water viscosity (μ), membrane area A_M , applied pressure ΔP and membrane resistance R_M will be investigated in this section. Eqs. (11) and (12) were used in this study by fixing the defined reference parameters and varying the target parameters one by one.

4.3.1. Fouling potential and particle concentration

The effects of different fouling mechanisms on the SDI will be demonstrated. Besides that, the influence of the main four fouling mechanisms on SDI results will be compared using Eqs. (11) and

Table 2
 $w_{(R,A,V)}$ values for each fouling mechanism.

Details	m	Fouling potential	$w_{(R,A,V)}$ [m] values for SDI = 3
Cake filtration	0	w_{RO}^a	12.2
Intermediate blocking	1	w_{AO}	17.5
Standard blocking	1.5	w_{VO}	40.5
Complete blocking	2	w_{AO}	24.3

^aCorresponding to $R_c = 1.06 \times 10^9 \text{ m}^{-2}$.

(12). The value of parameter m (0, 1, 1.5 or 2) indicates the fouling mechanism. For each fouling mechanism (or m value), the feed fouling parameters $w_{(R,A,V)}$ were determined for SDI=3. Table 2 shows the $w_{(R,A,V)}$ values for each of the four fouling mechanisms.

The sensitivity of the SDI to the feed fouling potential was studied as follows. By assuming $w_{(RO,AO,VO)}$ in Table 2 are the 100% values, the $w_{(RO,AO,VO)}$ values were varied in small steps between 40% and 180% of this value. Subsequently the ratios of the $w_{(R,A,V)}$ to $w_{(RO,AO,VO)}$ values were plotted in Fig. 3(a) and (b), which shows the sensitivity of SDI for $w_{(R,A,V)}$ and particle concentration for the different m values. $w_{(R,A,V)}$ by definition is inversely proportional to particle concentration.

As expected, the fouling potential $w_{(R,A,V)}$ is inversely related to the SDI: the lower the fouling potential $w_{(R,A,V)}$, the higher the SDI. The particle concentration is non-linearly related to the SDI shown in Fig. 3(b). However, the ideal fouling index should have a linear relationship to the particle concentration. The SDI sensitivity due to an increase in the fouling potential is higher if the complete blocking dominates the fouling mechanism. SDI is less sensitive if cake filtration is the main fouling mechanism.

4.3.2. Feed water viscosity (μ)

To investigate the sensitivity of the SDI for feed water viscosity, the feed temperature was varied between 5 and 50 °C. By changing the feed temperature, the feed water viscosity is affected. The effect of the temperature on the membrane properties (pore size, etc.) was neglected. In practice, the feed water temperature in desalination plants does not exceed 45 °C. Fig. 4(a) and (b) shows the effect of the feed water viscosity and feed water temperature on SDI results. The figures show that the temperature clearly influences the SDI value. The sensitivity of the SDI for temperature is higher under a pore blocking mechanism than with cake filtration.

4.3.3. Applied pressure (ΔP)

The applied pressure is the driving force during the SDI test. According to the ASTM standard, SDI tests require an applied constant pressure $207 \pm 7 \text{ kPa}$. Eqs. (11) and (12) were used to study the effect of the applied pressure on SDI results. Standard reference parameters were assumed and the applied pressure was varied between 0 and $4 \times 10^5 \text{ Pa}$ (0–4 bar). The calculated SDI was plotted vs. the assumed applied pressure in Fig. 5. The figure shows that the applied pressure influences the SDI measurement. SDI is more sensitive for a change in the applied pressure under the pore blocking mechanism than under the cake filtration mechanism.

4.3.4. Membrane resistance (R_M)

The membrane resistance is a membrane constant which does not depend on the feed composition nor on the applied pressure. Eqs. (11) and (12) together with the defined reference parameters and $w_{(R,A,V)}$ values in Table 2 were used to calculate the SDI as a function of the membrane resistance. In Fig. 6, the calculated SDI results were plotted for different membrane resistances. The figure shows that for all 4 fouling mechanisms with increasing membrane resistance the measured SDI value decreases.

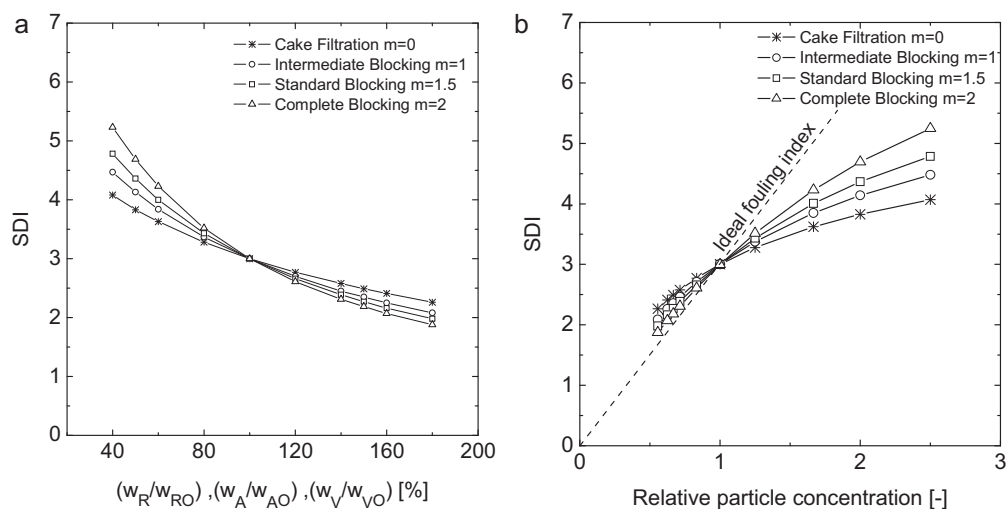


Fig. 3. The effect of different fouling mechanisms on the SDI. (a) SDI as a function of w_R , w_A and w_V . (b) SDI as a function of the particle concentration. Assuming the reference parameters, Eqs. (11) and (12) were used for calculating the SDI values for different fouling potentials and different fouling mechanisms.

4.4. Experimental results

To validate the model, SDI tests were performed for model feed waters with different feed water temperatures, applied pressures and AKP-15 particle concentrations. The experimental results will be compared to the modeling results. In this way, the limitations of the modeling will be studied.

4.4.1. Feed water temperature

Using the mathematical model in Eqs. (11) and (12), the effect of the feed water temperature (this section) and the applied pressure (Section 4.4.2) will be calculated theoretically and compared to the experimental data. The membrane resistance was defined as a model parameter equal to the initial resistance at $t=0$ and was corrected for temperature.

SDI-theory was calculated assuming a cake filtration mechanism. Reference parameters assumed were t_f 900 s, V_1 and V_2 0.1415 L, ΔP 207 kPa, and A_M $3.46 \times 10^{-4} \text{ m}^2$.

The fouling potential index I is a function of the dimension and nature of the particles and directly correlated to particle concentration [11]. Thus, I is independent of feed temperature and membrane resistance. For calculating SDI-theory, I was set as $3.06 \times 10^9 \text{ m}^{-2}$, the average value for 4 mg/L AKP-15.

The effect of the temperature on SDI results was assumed to be only due to a change in the feed water viscosity. Using the standard membrane M7, SDI was measured for different feed water temperature for 4 mg/L of AKP-15 (α -alumina) particle solution. The feed water temperature was controlled in the feed tank at three different temperatures (8, 21 and 38 °C) and the results are shown in Fig. 7.

Increasing the feed water temperature by 30 °C leads to decrease of the water viscosity by 50% and an increase in SDI of 82%. Fig. 7 shows that the relationship between SDI and temperature is non-linear.

SDI-measured is matching with SDI-theory at high temperature. However, at low temperature, SDI-theory is lower than SDI-measured by 0.9. Some measurement errors may occurred dur-

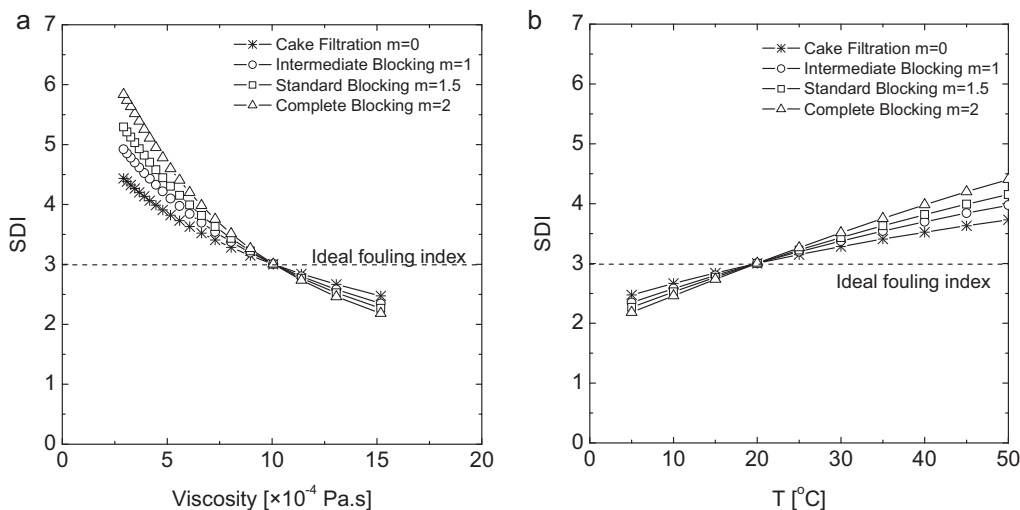


Fig. 4. The effect of the feed viscosity on SDI results. (a) SDI as a function of feed water viscosity, (b) SDI as a function of feed water temperature. Assuming the reference parameters, Eqs. (11) and (12) were used to calculate SDI values for different fouling mechanisms. The viscosity was varied between $(2.5 \text{ and } 15) \times 10^{-4} \text{ Pa.s}$ by varying the feed temperature between 5 and 50 °C.

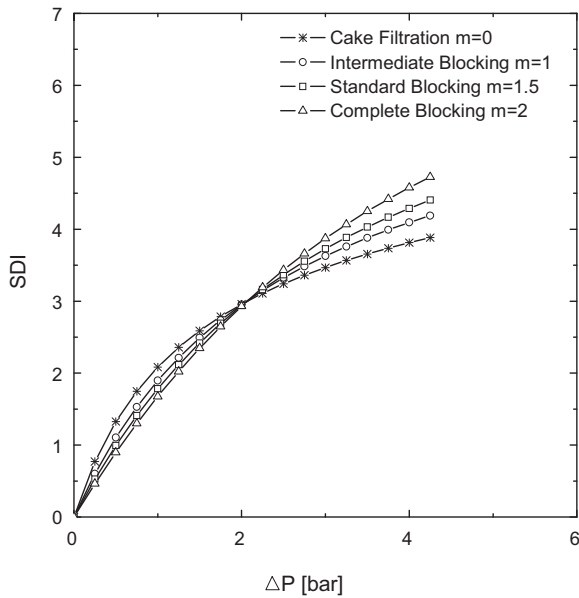


Fig. 5. The effect of the applied pressure on SDI results. Assuming the reference parameters, Eqs. (11) and (12) were used to calculate SDI values for different fouling mechanisms. The applied pressure was varied from 0 to 4×10^5 Pa (0–4 bar).

ing the test which affects the SDI value. The sensitivity for error is higher at low temperature than at high temperature [20]. However, the foulant–foulant and foulant–membrane interaction was not cooperated in the SDI-theory calculation to the effect of different fouling mechanisms occurs [20,21].

4.4.2. Applied pressure

Using the procedure described in Section 4.4.1, the effect of applied pressure difference on the SDI was determined theoretically and experimentally. Increasing the applied pressure leads to a larger amount of foulants arriving to the membrane surface in the same time frame. This increase in the fouling load leads to

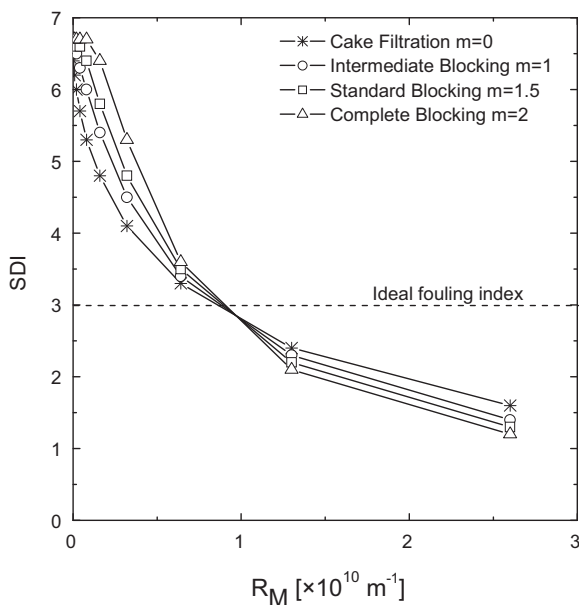


Fig. 6. The effect of the membrane resistance on SDI results. Assuming the reference parameters, Eqs. (11) and (12) were used to calculate SDI values for different fouling mechanisms. The membrane resistance was varied from 0 to 2.75×10^{10} m⁻¹.

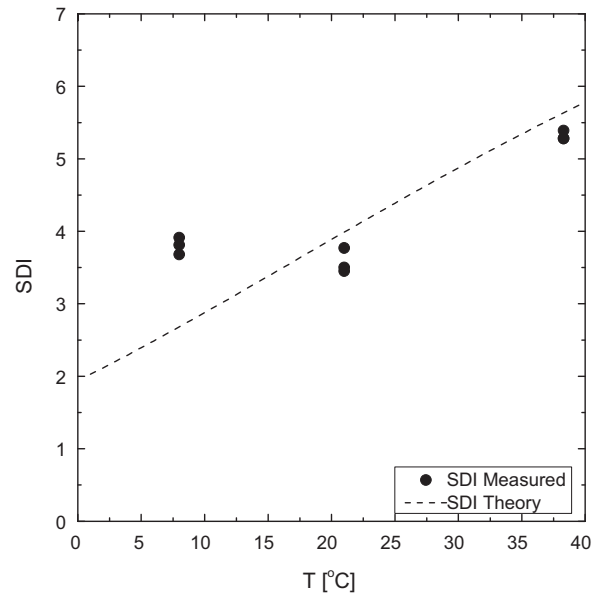


Fig. 7. SDI-measured and SDI-theory for different feed water temperatures (8, 21 and 38 °C) for a 4 mg/L AKP-15 feed solution using M7.

an increase in SDI. Fig. 8 shows the SDI-measured and SDI-theory results using a 4 mg/L of AKP-15 solution using M 7.

Fig. 8 shows that with increasing applied pressure the SDI increases significantly. The nonlinear relationship between SDI and the applied pressure is due to the fact that the SDI has a maximum value of 6.6. The SDI-measured and SDI-theory results are in good agreement.

4.4.3. SDI test for different particle concentration

Different concentrations of α -alumina (AKP-15) particles in ultra-pure water were prepared (0, 2, 4, 6, 8 and 10 mg/L). Three SDI tests were carried out for each concentration using the cellulose acetate MF membrane M7. In order to determine the parameters C, m and R_M , the best fits were calculated for the raw data (w and R) assuming one single fouling mechanism. The mathematical Eqs.

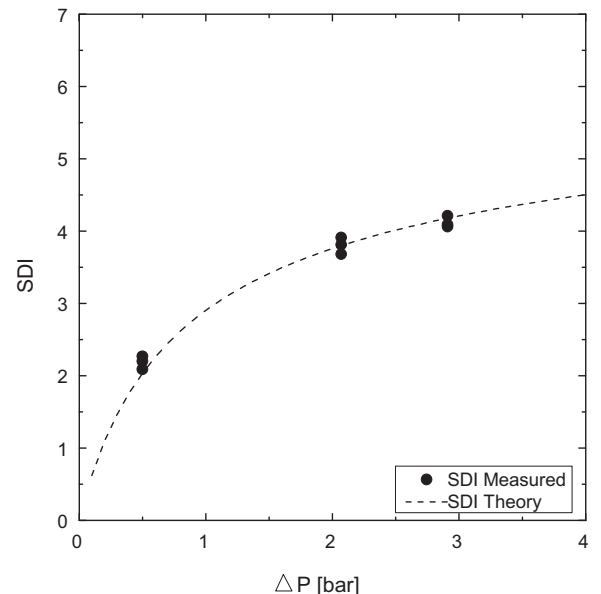


Fig. 8. SDI-measured and SDI-theory for different applied pressures (50, 207 and 290 kPa) for a 4 mg/L AKP-15 solution using M7.

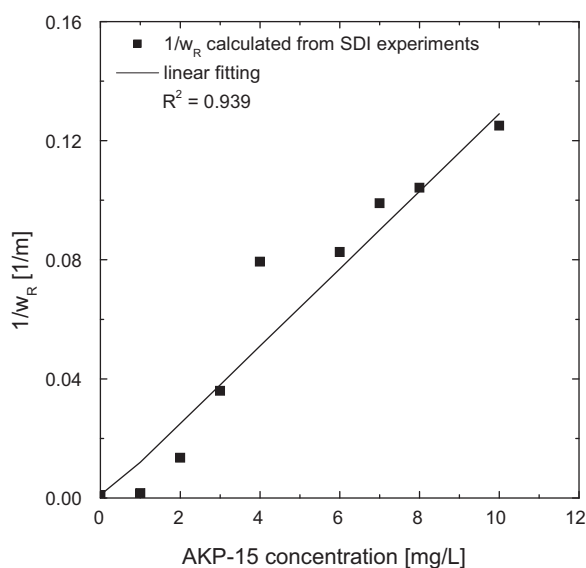


Fig. 9. w_R calculated from the SDI test and least square linear fitting. The fitting values of w_R are used in Eqs. (11) and (12) to determine the theoretical SDI values.

(11) and (12) and the measured testing parameters (T , ΔP and R_M) were used to calculate t_1 , t_2 and the SDI.

To determine the theoretical SDI values for different particle concentrations, the following procedure was applied. Assuming that cake filtration is the dominating fouling mechanism during the SDI measurements, w_R values obtained from the experimental data were plotted vs. the particle concentration in Fig. 9. Theoretically, the relation between w_R and the particle concentration is linear. However, the experimental w_R values show some deviations from this linearity. Therefore, a linear equation was fitted to the experimental data and w_R values were recalculated for each concentration (' w_R theory') using this linear least square fitting equation. Subsequently, the ' w_R theory' values were used to determine the theoretical SDI.

The measured values for t_1 , t_2 and the SDI were compared with the mathematically calculated values in Figs. 10 and 11. The maximum deviation between the calculated and measured values of t_1 and t_2 is indicated by dotted lines in Fig. 10.

The time required for collecting the first sample t_1 and the second sample t_2 were measured experimentally and estimated mathematically for each SDI test. In Fig. 10, the calculated t_1 and t_2 values are in good agreement with the measured values. There is some deviation due to the limitations of the model, which will be discussed in Section 4.4. The SDI test was performed for feed water prepared with different AKP-15 particle concentrations between 0 and 10 mg/L. The SDI as experimentally measured and the SDI values calculated using Eqs. (11) and (12) were plotted in Fig. 11.

The fouling potential of the feed water increases with increasing particle concentration. Since the particle retention in our work is 100%, the SDI increases exponentially when the particle concentration is higher [22]. In Fig. 11, the SDI has negative values at very low particle concentrations, which can be explained by the high sensitivity of the SDI for measurement errors in this region. Deviations between the calculated and the measured SDI values can be explained by the limitations of the model as will be discussed in Section 4.6.

4.5. Fouling load

The SDI test essentially determines the average flow during filtration of a reference volume. The change in average flow between the two measurements (represented by t_1 and t_2) is a measure

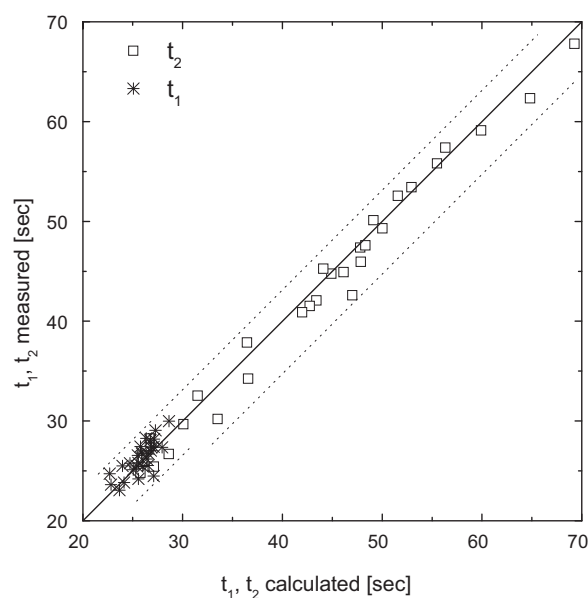


Fig. 10. Calculated and measured times to collect the first (t_1) and the second samples (t_2) for different particle concentrations. Calculated t_1 and t_2 were determined using Eqs. (11) and (12) and the measured testing parameters T , A_M , ΔP and R_M . Measured t_1 and t_2 were determined according to the ASTM standard protocol.

for the change in the fouling state of the test membrane. In the fouling models the fouling state of the membrane is related to the filtered volume. However, in the SDI test the time between the two measurements is fixed and the total volume that is filtered in that time depends on the flow rate. Thus, any effect that increases the flow through the membrane will increase the fouling load of the membrane incrementally and consequently the measured SDI will be higher. This explains our observation that the SDI increases with increasing temperature (decreasing viscosity implies increased flow), increasing pressure and decreasing membrane resistance.

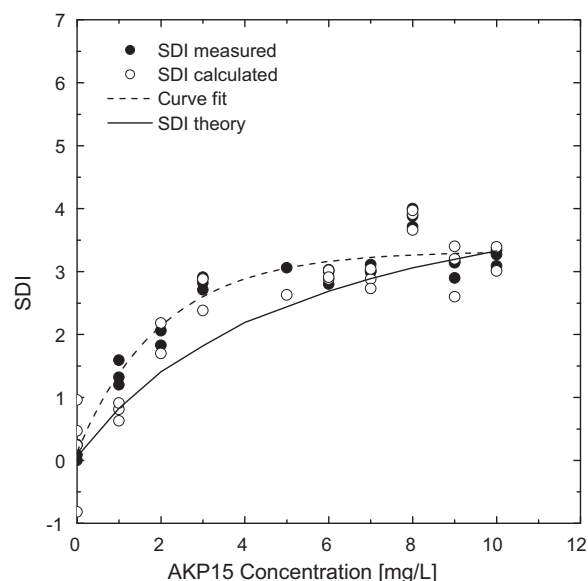


Fig. 11. Calculated, measured and theoretical SDI values. Calculated SDI results were determined using Eqs. (11) and (12) and the measured parameters T , A_M , ΔP and R_M . Theoretical SDI values were calculated assuming cake filtration and the expected C and m values for AKP-15. Measured SDI values were determined according to the ASTM standard.

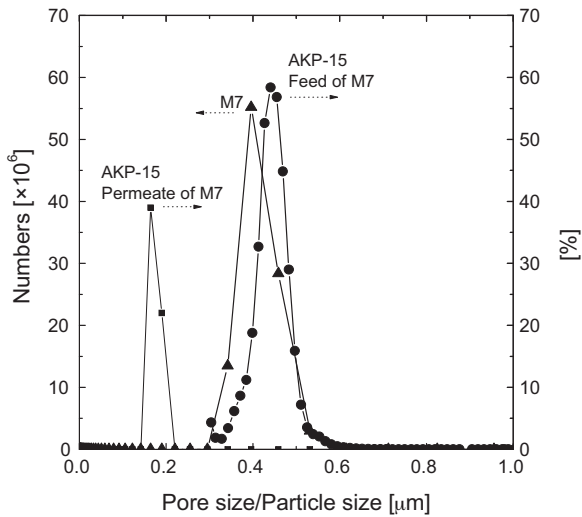


Fig. 12. α -Alumina (AKP-15) particle size distribution (4 mg/L particles in ultra-pure water at pH 4.1 and T 20 °C well mixed) determined using a Malvern Zetasizer feed and permeate of M7. The pore size distribution for membrane M7 is measured using the Coulter Porometer II with Porofl3 as pore filling liquid.

The plugging ratio is corresponding to the change in the resistance during the SDI test. Eq. (4) shows that the relation between the filtered volume and the fouling resistance and thus the flow decline is non-linear. The sensitivity of the fouling resistance due to the change in the filtrated volume is increased with increasing m value (0, 1, 1.5 and 2). Hence, when this relation is convex, a moderate increment in filtered volume can result in a relatively large increase in the fouling resistance. As a result, the sensitivity for factors that increase flow is also relatively large. This explains our observation that the cake filtration mechanism (lowest m value) is the least sensitive for the testing conditions, followed by intermediate blocking, standard blocking and complete blocking. Consequently, the sensitivity of the SDI increases in the same order: cake filtration < intermediate blocking < standard blocking < complete blocking.

The amount of foulants required for increasing the resistance with a certain value ΔR in case of pore blocking is less than the amount of foulants required for the same increase in the resistance in case of cake filtration. Since the testing conditions influence the fouling load arriving to the membrane surface, the sensitivity of SDI (for the testing conditions) is higher if the pore blocking is the dominant mechanism.

4.6. Shortcomings of the model

The deviations between the measured and calculated SDI values can be explained in different ways. The commercial 0.45 μm membranes which are used for SDI test actually have a broad pore size distribution (Fig. 12). Furthermore, Fig. 12 shows that the α -alumina particles have a particle size distribution between 200 and 800 nm with an average size of 600 nm. During the SDI test, the smaller particles either will deposit deeply in the pores and cause pore blocking, or will pass to permeate side. The cake layer formation will start when enough large particles arrived to the membrane surface. So, one or more fouling mechanisms can occur during the SDI test in parallel or successively. Flux decline can be consistent with one or more pore blocking mechanisms during the earlier stages and with the cake filtration mechanism during the latest stages of filtration [23].

1. Feed water properties such as pH and salinity influence the foulant–foulant and foulant–membrane interactions by affect-

ing the surface charge of both particle and membrane. The change in the surface charge can influence the membrane adsorption for particles (standard pore blocking) as well as the cake layer density. The fouling rate will be influenced too and that is reflected by the SDI value. The feed water temperature can influence the SDI by a change in the water viscosity. In Eqs. (11) and (12) the effect/s of the feed temperature on the membrane physical properties was neglected.

2. A particle rejection of 100% was assumed in de modeling. However, small particles were noticed in the permeate of M7 indicating that the particle rejection is below 100%.

5. Conclusions

The SDI measurement initially is designed to measure the fouling potential of feed water for RO membranes. However, the measured values will also depend on several testing parameters. In this paper a mathematical fouling model based on blocking laws was further extended, which is able to explain this dependency and shows why a reproducible determination of the SDI is difficult.

An increase in testing parameters such as T , ΔP or R_M affect the fouling load, which leads to a different SDI value. The sensitivity of the SDI for small variations in the testing parameters increases when the relation between w and R is stronger, so in the order cake filtration < intermediate blocking < standard blocking < complete blocking.

An increase of the feed water viscosity or the membrane resistance leads to a decrease in the SDI, while an increase of the applied pressure or the feed temperature leads to an exponential increase of the SDI. The membrane area has no effect on SDI as far as the sample volume is adjusted proportionally to the membrane area.

The relation between the particle concentration and the SDI is a function of the fouling mechanism parameter m . Therefore, for the same amount of particles in the feed, the SDI can vary depending on the fouling mechanisms occurring during the test.

The experimental and calculated SDI values are in good agreement with the results of the mathematical modeling. An ideal fouling index should have a linear relationship with the relevant particle concentration in the feed water and should not be sensitive for the testing condition parameters nor the membrane resistance. The final conclusion of this work is that the SDI is not an ideal fouling index due to the influence of the membrane resistance and the testing condition parameters on the measured values. Moreover, the SDI has no linear relationship with the fouling potential (particle concentration). Therefore, there is a strong need for normalization of the SDI which compensates for variations in these parameters.

Acknowledgements

The authors of the paper would like to acknowledge the scientific and financial support of Vitens and Norit Process Technology B.V./X-Flow B.V. Part of this work is carried out in the framework of the InnoWATOR subsidy regulation of the Dutch Ministry of Economic Affairs (project IWA08006 'Zero Chemical UF/RO System for Desalination').

Annex 1.

General SDI equation for $m \neq 1$ or 2

$$m = 0 \quad C = \frac{R_M}{wR}, \quad m = 1.5 \quad C = \frac{2}{wV R_M^{0.5}}$$

$$t_1 = \frac{(((V_1 \cdot C(1-m))/(R_M^{(1-m)} A_M) + 1)^{1/(1-m)} - 1)^{2-m}}{(2-m)C \cdot dP \cdot R_M^{(m-1)}}$$

$$t_2 = \frac{\left(\frac{((R_M^{1-m})((1+((2-m)C \cdot dP \cdot R_M^{(m-1)} t_{15})/(\mu \cdot R_M))^{1/(2-m)} - 1)A_M)) / (C(1-m)) + V_2) C(1-m)}{(R_M^{(1-m)} A_M + 1)^{1/(1-m)}} \right)^{2-m} - 1}{(2-m)C \cdot dP \cdot R_M^{(m-1)}} - t_{15}$$

General SDI equation for $m = 1$

$$C = \frac{1}{w_A}$$

$$t_1 = \frac{(e^{(V_1)/(A_M \cdot w_A)} - 1) R_M \cdot w_A \cdot \mu}{dP}$$

$$t_2 = \frac{\ln(-1/ - (1/(e^{(dP \cdot t_{15})/(R_M \cdot w_A \cdot \mu)} - 1) A_M \cdot w_A + V_2)/(A_M \cdot w_A + 1) R_M \cdot w_A \cdot \mu - t_{15}}{\ln(e) \cdot dP} - t_{15}$$

General SDI equation for $m = 2$

$$C = \frac{1}{R_M w_A}$$

$$t_1 = \frac{\ln(1/(-V_1/A_M \cdot w_A + 1)) R_M \cdot w_A \cdot \mu}{\ln(e) \cdot dP}$$

$$t_2 = \frac{\ln(1/(-((1/e^{(dP \cdot t_{15})/(R_M \cdot w_A \cdot \mu)} - 1) A_M \cdot w_A + V_2)/(A_M \cdot w_A + 1) R_M \cdot w_A \cdot \mu - t_{15}}{\ln(e) \cdot dP} - t_{15}$$

Nomenclature

A_M	membrane area [m ²]
A_{M0}	reference membrane area 13.4×10^{-4} [m ²]
C	scaling factor proportional to the foulants concentration
ΔP	applied pressure [Pa]
ΔP_0	reference applied pressure 207 [kPa]
J	flux [m ³ /m ² s bar]
J_0	initial flux [m ³ /m ² s bar]
m	fouling mechanism parameter (0, 1, 1.5 and 2)
n	number of data points
%P	plugging ratio [%]
R	total resistance [m ⁻¹]
R_C	specific cake resistance [m ⁻²]
R_M	membrane resistance [m ⁻¹]
R_{M0}	reference membrane resistance 1.29×10^{10} [m ⁻¹]
R_i	total resistance at data point i
SDI	Silt Density Index [%/min]
s	operating strategy parameter (0, 1 and 0.5)
$t_{1,2}$	time to collect the first and second sample [s]
t_f	elapsed filtration time 15 [min] or 900 [s]
T	temperature [°C]
T_0	reference temperature 20 [°C]
V	filtered volume [m ³]
$V_{1,2}$	sample volume [m ³]
$w_{R,A,V}$	fouling potential [m]
w	filtrated state [m]
w_i	local accumulated filtrated volume at data point i

Greek letters

μ	viscosity [Pa s]
γ	difficulty of operation due to fouling

References

- [1] S. Lee, J. Cho, M. Elimelech, Combined influence of natural organic matter (NOM) and colloidal particles on nanofiltration membrane fouling, *Journal of Membrane Science* 262 (2005) 27–41.
- [2] S. Lee, J. Cho, M. Elimelech, Influence of colloidal fouling and feed water recovery on salt rejection of RO and NF membranes, *Desalination* 160 (2004) 1–12.
- [3] J.S. Baker, L.Y. Dudley, Biofouling in membrane systems – a review, *Desalination* 118 (1998) 81–89.
- [4] J.S. Vrouwenvelder, S.A. Manolarakis, H.R. Veenendaal, D. van der Kooij, Biofouling potential of chemicals used for scale control in RO and NF membranes, *Desalination* 132 (2000) 1–10.
- [5] P.A.C. Bonn e, J.A.M.H. Hofman, J.P. van der Hoek, Scaling control of RO membranes and direct treatment of surface water, *Desalination* 132 (2000) 109–119.
- [6] K.O. Agenson, T. Urase, Change in membrane performance due to organic fouling in nanofiltration (NF)/reverse osmosis (RO) applications, *Separation and Purification Technology* 55 (2007) 147–165.
- [7] S.F.E. Boerlage, M. Kennedy, M.P. Aniye, J.C. Schippers, Applications of the MFI-UF to measure and predict particulate fouling in RO systems, *Journal of Membrane Science* 220 (2003) 97–116.
- [8] A. Nahrstedt, J. Camargo-Schmale, New insights into silt density index and modified fouling index measurements, in: IWA2008, San Francisco, USA, 2008.
- [9] ASTM Standard (D 4189 – 07): Standard Test Method for Silt Density Index (SDI) of Water, D19.08 on Membranes and Ion Exchange Materials, 2007.
- [10] J.C. Schippers, J. Verdouw, The modified fouling index, a method of determining the fouling characteristics of water, *Desalination* 32 (1980) 137–148.
- [11] S.F.E. Boerlage, M.D. Kennedy, M.P. Aniye, E.M. Abogrean, G. Galjaard, J.C. Schippers, Monitoring particulate fouling in membrane systems, *Desalination* 118 (1998) 131–142.
- [12] J.C. Schippers, J.H. Hanemaayer, C.A. Smolders, A. Kostense, Predicting flux decline of reverse osmosis membranes, *Desalination* 38 (1981) 339.
- [13] S.F.E. Boerlage, M.D. Kennedy, P.A.C. Bonne, G. Galjaard, J.C. Schippers, Prediction of flux decline in membrane systems due to particulate fouling, *Desalination* 113 (1997) 231–233.
- [14] S.F.E. Boerlage, M.D. Kennedy, M.P. Aniye, E. Abogrean, Z.S. Tarawneh, J.C. Schippers, The MFI-UF as a water quality test and monitor, *Journal of Membrane Science* 211 (2003) 271–289.
- [15] J. Hermia, Constant pressure blocking filtration laws – application to power-law non-newtonian fluids, *Transactions on IChemE* 60 (1982) 183–187.
- [16] B. Blankert, B.H.L. Betlem, B. Roffel, Dynamic optimization of a dead-end filtration trajectory: blocking filtration laws, *Journal of Membrane Science* 285 (2006) 90–95.
- [17] M. Mulder, *Basic Principles of Membrane Technology*, 2nd ed., Kluwer Academic Publishers, Dordrecht, The Netherlands, 2003.
- [18] C.R. Rao, H. Toutenburg, A. Fieger, C. Heumann, T. Nittner, S. Scheid, *Linear Models: Least Squares and Alternatives*, Springer, New York, 1999.
- [19] F. Rosignol, A.L. Penard, F.H.S. Nagaraja, C. Pagnoux, T. Chartier, Dispersion of alpha-alumina ultrafine powders using 2-phosphonobutane-1,2,4-tricarboxylic acid for the implementation of a DCC process, *European Ceramic Society* 25 (2005) 1109–1118.
- [20] A. Alhadidi, B. Blankert, A.J.B. Kemperman, J.C. Schippers, M. Wessling, W.G.J. van der Meer, Sensitivity of SDI for the error in measuring the testing parameters, *Desalination and Water Treatment* (2011). Under revision.
- [21] A. Alhadidi, A.J.B. Kemperman, J.C. Schippers, M. Wessling, W.G.J. van der Meer, Silt density index and modified fouling index relation, and effect of pressure, temperature and membrane resistance, *Desalination* 273 (2011) 48–56.
- [22] L.F. Greenlee, D.F. Lawler, B.D. Freeman, B. Marrot, P. Moulin, Reverse osmosis desalination: water sources, technology, and today's challenges, *Water Research* 43 (2009) 2317–2348.
- [23] F. Wang, V.V. Tarabara, Pore blocking mechanisms during early stages of membrane fouling by colloids, *Journal of Colloid and Interface Science* 328 (2008) 464.